A variational study of donors in quantum wires in an external magnetic field

1996 J. Phys.: Condens. Matter 8 10521

(http://iopscience.iop.org/0953-8984/8/49/039)

J. Phys.: Condens. Matter **8** (1996) 10521–10531. Printed in the UK

A variational study of donors in quantum wires in an external magnetic field

T Szwacka

Departamento de Física, Facultad de Ciencias, Universidad de Los Andes, Mérida, Venezuela

Received 18 June 1996

Abstract. We present the results of systematical variational investigations of the ground and $2p^-$ states of D^0 centre in a rectangular quantum wire. The objective was to find the general trends for the donor binding energy and the dipole optical transition energy with changing transversal dimensions of the wire and the external magnetic field perpendicular to the wire. Simple Gaussian-like trial envelope functions and variable gauge of the vector potential were used in variational calculations. Besides, we investigated a donor impurity in quantum wires with parabolic confinements and the correspondence of such wires and rectangular quantum wires in the case of donor impurities.

1. Introduction

There is a great deal of interest in quantum wires [1–12], i.e. quasi-one-dimensional systems, whose physical properties have quite new aspects in comparison to those observed in bulk materials and two-dimensional systems. The visible progress in crystal growth and fabrication techniques to obtain such systems has inspired numerous theoretical studies of optical and transport properties, electronic structure and excitonic and impurity levels. In the case of an impurity states the effects of several factors on impurity spectra have been investigated: the height of the potential barriers, the shape of the wire's cross section, the transversal dimensions of the wire, the position of the impurity centre with respect to the axis of the wire and the external magnetic field acting along the wire or in the direction perpendicular to it [13–24]. Besides, problems related to the boundary conditions, the effect of image potential on the impurity states and polarizabilities of shallow donors were considered [25–28]. Most of the calculations were performed for a hydrogenic impurity in the effective-mass approximation, within the variational approach, so the theoretical investigations of the impurity states in quantum wires cover quite similar subjects as in the case of quantum wells but as different authors concentrated on different aspects of the problem the results are rather scattered and the general trends are not easy to trace. Though impurities in quantum wires were observed recently in experiment [10, 11, 29] very sophisticated calculations of the fine details of the impurity spectra with complicated trial wavefunctions requiring a lot of computational effort (more than for the similar problem in the case of an impurity in a quantum well) seem to be premature. At present, the most profitable and useful studies for the experimental search for the signature of impurities in quantum wires seem to be rather systematic theoretical studies of the behaviour of the impurity states with the changes of principal wire parameters. This goal can be achieved with the use of rather simple variational trial functions requiring a minor computational effort.

0953-8984/96/4910521+11$19.50

Our experience with variational calculations of the D^0 spectra in bulk semiconductors and quantum wells [30, 31] suggests that very simple Gaussian bases give quite accurate results in the case of moderate and strong magnetic fields.

The purpose of the present paper is to investigate systematically the changes of the ground and $2p^-$ states of a D^0 centre placed at the axis of a rectangular wire with changing transversal dimensions of the wire and the external magnetic field in the direction perpendicular to one of the sides of the rectangle. It is easy to see that such an external magnetic field differentiates between the effects of the two well potentials forming a quantum wire. The confinement effect of one of the wells acts together with the confining effect of the magnetic field. One may expect however that in limiting cases of the well widths, $l_\perp$, and the magnetic fields the results will be mostly determined by one of the two factors. It is also rather natural to expect the essential effect of the change of the width of the other well, $l_\parallel$ (which is in the direction of the magnetic field), to consist primarily in the uniform vertical shift of the curves representing the dependence of the binding energy, E_D (or 1s–$2p^-$ transition energy, ΔE), on a magnetic field, for fixed $l_\perp$. An impurity in a quantum wire in a magnetic field represents a very complex system, so that the verification of these qualitative expectations may only come from numerical results.

We shall investigate also the ground and $2p^-$ states of a D^0 centre in a quantum wire with parabolic confinements. Correspondence between such wires and rectangular quantum wires is expected.

In section 2 we present the calculated binding energies of a donor impurity and in section 3 we concentrate on the energy of the dipole optical transition expected for infrared radiation with the electric field parallel to the wire.

2. The ground state of a donor impurity in the quantum well wire

Let us take the axis of the quantum wire along the x-direction and the magnetic field $\boldsymbol{B}$ perpendicular to the wire in the z-direction. Then the wire cross section will be in the yz plane with the dimensions $l_\perp$ along the y axis and $l_\parallel$ along the magnetic field. This wire structure can be obtained as a superposition of two square-well potentials which can be written in the form

$$V_1(y) = \begin{cases} 0 & \text{for } |y| < l_\perp/2 \\ V_0 & \text{for } |y| > l_\perp/2 \end{cases} \qquad V_2(z) = \begin{cases} 0 & \text{for } |z| < l_\parallel/2 \\ V_0 & \text{for } |z| > l_\parallel/2 \end{cases} \tag{1}$$

where V_0 denotes the barrier height (for GaAs well sandwiched by $Ga_{1-x}Al_xAs$ barriers, $V_0 = 0.65 \times 1.247x$ eV [32]). We shall consider the case when the donor impurity is placed on the axis of the wire. The magnetic field $\boldsymbol{B}$ in the z-direction can be described by the vector potential in the form

$$\boldsymbol{A} = [-\alpha By, (1-\alpha)Bx, 0] \tag{2}$$

where $0 \leqslant \alpha \leqslant 1$ will play the role of one of the variational parameters involved in the problem. It will be shown that the presence of the parameter α in (2) can be quite important when rather simple variational trial wavefunctions are used. It is known [33] that if the variational wavefunction is not very flexible (involves only few variational parameters) the gauge of the vector potential plays an important role.

The dimensionless effective mass Hamiltonian for our system, with the vector potential described by (2), has the form

$$H = H_0 - 2/r \tag{3}$$

where H_0 represents the Hamiltonian of the free electron in the quantum wire in the presence of a magnetic field

$$H_0 = -\nabla^2 + (2/\mathrm{i})\gamma[(1-\alpha)x(\partial/\partial y) - \alpha y(\partial/\partial x)] + (1-\alpha)^2\gamma^2x^2 + \alpha^2\gamma^2y^2 + V_1(y) + V_2(z) \tag{4}$$

where $V_1(y)$ and $V_2(z)$ are given by (1). The energy is measured in effective Rydbergs $\mathrm{Ryd}^* = m^*e^4/2\bar{h}^2\varepsilon^2$, and the effective Bohr radius $a_B^* = \bar{h}^2\varepsilon/m^*e^2$ is the unit of the distance ($-e$ and m^* are the charge and effective mass of an electron, respectively, and ε the static dielectric constant). The parameter $\gamma = \bar{h}\omega_c/2\ \mathrm{Ryd}^*$ is a measure of the magnetic field ($\bar{h}\omega_c$ being the cyclotron energy).

We propose the following variational trial wavefunction for the electron bound to the impurity [described by the Hamiltonian (3)]

$$\Psi = N\exp(-\lambda x^2 - \mu y^2 - \nu z^2) f_1(y) f_2(z). \tag{5}$$

Here λ, μ, and ν are variational parameters for the Gaussian-like envelope wavefunction while $f_1(y)$ and $f_2(z)$ are the ground-state eigenfunctions of the square-well potentials $V_1(y)$ and $V_2(z)$, respectively, and N is the normalization constant. In the case of a free electron when the magnetic field is absent there exists the exact solution for the lowest-energy 1D subband for a free electron:

$$\psi_{0k_x} = \left(1/\sqrt{L_x}\right)\exp(\mathrm{i}k_x x) f_1(y) f_2(z) \tag{6}$$

where L_x is the length of the wire. The bottom of the subband corresponds to the $k_x = 0$ state with the wavefunction ψ_0. In the presence of the magnetic field parallel to the z-axis and the Landau gauge with $\alpha = 1$ the eigenfunction of the lowest-energy state has the product form (N' being the normalization constant)

$$\psi = N' g_1(y) f_2(z) \tag{7}$$

but $g_1(y)$ cannot be found analytically. We use for $g_1(y)$ the trial function of the form

$$g_1(y) = \exp(-\mu' y^2) f_1(y). \tag{7a}$$

For a general gauge with $\alpha \neq 1$ we used the free electron trial wavefunction

$$\psi = N' \exp(-\lambda' x^2 - \mu' y^2) f_1(y) f_2(z) \tag{8}$$

and we have proved that for a free electron the Landau gauge with $\alpha = 1$ is the preferential one.

The binding energy of the donor impurity ground state is given by the difference of two energy expectation values

$$E_B(\gamma) = \langle\Psi|H|\Psi\rangle - \langle\psi|H_0|\psi\rangle \qquad \text{for } \gamma \neq 0 \tag{9}$$

and

$$E_B(\gamma = 0) = \langle\Psi|H|\Psi\rangle - \langle\psi_0|H_0|\psi_0\rangle \qquad \text{for } \gamma = 0. \tag{10}$$

We have the analytical expression only for the expectation value $\langle\psi_0|H_0|\psi_0\rangle = E_1 + E_2$, where E_1 and E_2 are the energies of the bottoms of the lowest subbands for an electron in the quantum well given by $V_1(y)$ and $V_2(z)$, respectively, in the absence of the magnetic field. The other expectation values have the following expressions:

$$\langle\Psi|H|\Psi\rangle = \langle\Psi|H_0|\Psi\rangle - 2N^2\int_{-\infty}^{+\infty}\mathrm{d}x\int_{-\infty}^{+\infty}\mathrm{d}y\int_{-\infty}^{+\infty}\mathrm{d}z\,\frac{f_1^2(y)f_2^2(z)}{\sqrt{x^2+y^2+z^2}} \times \exp[-2(\lambda x^2 + \mu y^2 + \nu z^2)] \tag{11}$$

where

$$\langle\Psi|H_0|\Psi\rangle = E_1 + E_2 + \lambda + \frac{(1-\alpha)^2\gamma^2}{4\lambda} - \frac{1}{2}(4\mu^2 + \alpha^2\gamma^2)\frac{\mathrm{d}}{\mathrm{d}\mu}(\ln I_1(\mu)) \\ -2\nu^2\frac{\mathrm{d}}{\mathrm{d}\nu}(\ln I_2(\nu)) \tag{12}$$

and

$$N^{-2} = [\pi^{1/2}/(2\lambda)^{1/2}]I_1(\mu)I_2(\nu). \tag{13}$$

$I_1(\mu)$ and $I_2(\nu)$ represent the following integrals

$$I_1(\mu) = \int_{-\infty}^{+\infty} \mathrm{d}y\ f_1^2(y)\exp(-2\mu y^2) \tag{14}$$

$$I_2(\nu) = \int_{-\infty}^{+\infty} \mathrm{d}z\ f_2^2(z)\exp(-2\nu z^2). \tag{15}$$

The energy expectation value $\langle\psi|H_0|\psi\rangle$ for the free electron in the presence of an external magnetic field has the form

$$\langle\psi|H_0|\psi\rangle = E_1 + E_2 + \lambda' + \frac{(1-\alpha)^2\gamma^2}{4\lambda'} - \frac{1}{2}(4\mu'^2 + \alpha^2\gamma^2)\frac{\mathrm{d}}{\mathrm{d}\mu'}(\ln I_1(\mu')). \tag{16}$$

It is an interesting fact that with the trial function given by (8) the difference between the free electron values of the lowest energy level obtained for the Landau gauge ($\alpha = 1$) and for the symmetrical gauge ($\alpha = 0.5$) is quite big. For example for the quantum wire with $l_\perp = l_\parallel = 1\ a_B^*$ and for $\gamma = 5$ this difference represents about 11% of the free electron ground state energy.

All numerical calculations reported below were performed for a given height $V_0 = 34.9$ Ryd*. This corresponds to the composition $x = 0.25$ in the $Ga_{1-x}Al_xAs$ type barriers sandwiching the GaAs wire. Even though this height seems to be quite large, the result still differs considerably from the infinite-barrier case. For example, the difference between the binding energies obtained for $V_0 = 34.9$ Ryd* and for $V_0 = 119$ Ryd* (corresponding to the composition $x = 0.85$ in the $Ga_{1-x}Al_xAs$ type barriers) exceeds 10% (for an impurity on the axis of the wire for $\gamma = 0$).

In figure 1 we present the calculated binding energy of a D^0 centre on the axis of the quantum wire with square cross section ($l_\perp = l_\parallel = l$) for a quite wide range of magnetic fields. The magnetic field is perpendicular to a side of the square $l_\perp$. Five different cross sections with $l = 1$, 1.5, 2, 3 and 4 a_B^* were studied. To visualize better the general trends the bulk binding energy for the D^0 centre calculated within the same approximation is also plotted (dotted curve). We have checked that the relative accuracy of the one-Gaussian approximation, rather poor for the bulk case at low magnetic fields, improves considerably in the presence of strong confinement, whatever its origin. We can see from figure 1 that with the decrease of the transversal dimensions of a square quantum wire the visible magnetic confinement effect on the binding energy starts at higher and higher fields. The narrower the wire, the less sensitive is the binding energy to the external magnetic field.

In figures 2 and 3 we plot the calculated binding energy of a D^0 centre on the axis of a quantum wire with rectangular cross section, for the same region of the magnetic fields as in figure 1. In both figures the continuous curves correspond to fixed length of the side $l_\perp$ of the rectangle (in the direction perpendicular to the magnetic field). In figure 2 this fixed $l_\perp$ is equal to 1 a_B^* whereas the length of the rectangle side parallel to the magnetic field assumes subsequent values $l_\parallel = 0.5$, 1, 2, 4 and ∞ a_B^*. In figure 3 for continuous curves $l_\perp = 2\ a_B^*$ and for the other side we have chosen the values $l_\parallel = 1$, 2, 4 and ∞ a_B^*. We can

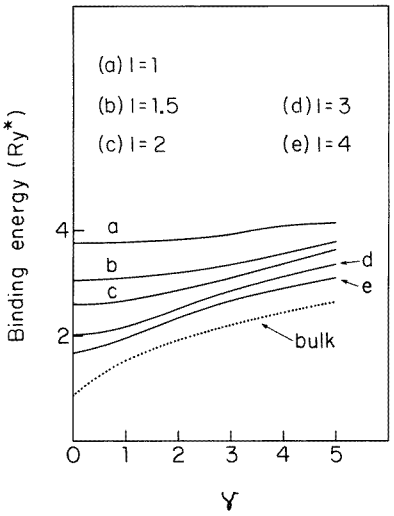

Figure 1. The binding energy of a D^0 centre on the axis of a quantum wire with square cross section ($l_\perp = l_\parallel = l$) as a function of the magnetic field, for various wires. The dotted curve corresponds to the case of the bulk binding energy.

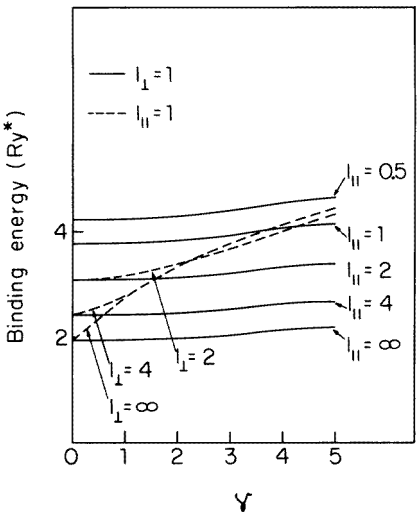

Figure 2. The binding energy of a D^0 centre on the axis of various quantum wires with rectangular cross section as a function of the magnetic field. The continuous curves correspond to the fixed length of the rectangle side $l_\perp = 1\ a_B^*$ and the broken curves correspond to the case of fixed $l_\parallel = 1\ a_B^*$.

see from figure 2 that for all continuous curves, even for $l_\parallel = \infty$, the D^0 binding energy depends only weakly on the magnetic field. This dependence becomes more pronounced for the bigger value of $l_\perp = 2\ a_B^*$ used in figure 3. In both cases (figure 2 and figure 3) the magnetic field dependence of the binding energy seems to be independent of $l_\parallel$. The essential effect of the change of $l_\parallel$ for fixed $l_\perp$ consists in the uniform vertical shift of the

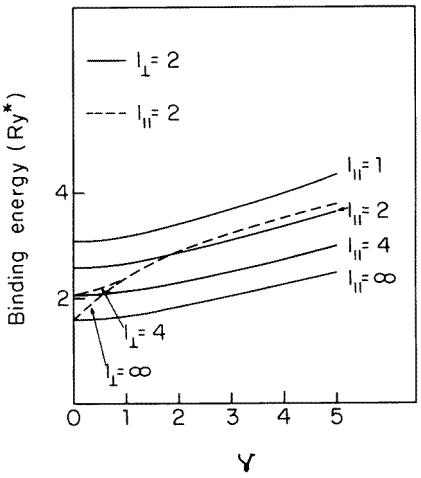

Figure 3. The binding energy of a D^0 centre on the axis of various quantum wires with rectangular cross section as a function of the magnetic field. The continuous curves correspond to the fixed length of the rectangle side $l_\perp = 2\ a_B^*$ and the broken curves correspond to the case of fixed $l_\parallel = 2\ a_B^*$.

curves. In spite of the fact that in the presence of the Coulomb potential the Schrödinger equation does not factorize the effect of $l_\parallel$ is field independent as for a free electron.

The broken curves in figures 2 and 3 correspond to the situation when the length of the rectangle side parallel to the magnetic field is fixed: $l_\parallel = 1\ a_B^*$ in figure 2 and $l_\parallel = 2\ a_B^*$ in figure 3. The lengths of the other side are $l_\perp = 2$, 4 and $\infty\ a_B^*$ for figure 2 and $l_\perp = 4$ and $\infty\ a_B^*$ for figure 3. We can see that for all broken curves the magnetic field effect on the D^0 binding energy is strong. The $l_\perp$-related confinement plays an important role only for small (and in some cases also moderate) magnetic fields determining, for example, together with the magnetic field the slope of the broken curves. For field high enough it becomes dominant: the slope of the binding energy curves is determined by the magnetic field only. All broken curves for fixed $l_\parallel$ value are nearly parallel to each other or even coincide in that region of γ. It is interesting to note that starting from some γ value the magnetic field perpendicular to the quantum well ($l_\perp = \infty$) can be more effective than the field in quantum wires (see figure 2).

Let us propose now parabolic confinements instead of the square-well potentials given by (1). In the direction y (perpendicular to the external magnetic field) we propose the parabolic-shaped potential in the form

$$V_{1p}(y) = \eta_\perp y^2 \tag{17}$$

instead of the potential $V_1(y)$ and in the direction of the magnetic field the parabolic potential

$$V_{2p}(z) = \eta_\parallel z^2 \tag{18}$$

instead of the potential $V_2(z)$. The energy of the lowest free electron state in the wire with parabolic confinements given by (17) and (18), in the presence of magnetic field in the z-direction, has an analytical expression given by

$$\sqrt{\eta_\parallel} + \sqrt{\eta_\perp + \gamma^2}. \tag{19}$$

The following variational trial wavefunction for the electron bound to the impurity was proposed:

$$\Psi' = N_p \exp(-\lambda x^2 - \mu y^2 - \nu z^2). \tag{20}$$

The numerical results of D^0 binding energy obtained in this case show the existence of correspondence between the parabolic confinement and the square-well confinement (at least for the case of D^0 binding energy). The same curves of the D^0 binding energy as a function of the magnetic field as plotted in figures 1–3 we can obtain with a proper substitution of square-well potentials by the parabolic ones. For the square well of any extension l (and any height) we can find a parabolic well defined by some η so that the binding energy of the D^0 centre on the axis of the wire structure obtained as a superposition of two square-well potentials differs by less than 1% from the D^0 binding energy in the wire obtained as a superposition of proper parabolic potentials, for the entire range of magnetic fields we considered. Of course the same occurs when we substitute only one of the square-well potentials by the proper parabolic one. The following correspondence between the parameters defining the square-well potential and the parabolic potential was obtained:

Table 1.

l	1	2	4
η	50	5.5	0.45

3. The $2p^-$-like excited state and optical transition energies

For the electron in the $2p^-$-like excited state of the neutral donor we propose the following variational wavefunction:

$$\Psi_1 = N_1(x + i\beta y) \exp(-\lambda_1 x^2 - \mu_1 y^2 - \nu_1 z^2) f_1(y) f_2(z). \tag{21}$$

Here λ_1, μ_1 and ν_1 are variational parameters of the Gaussian-like envelope wavefunction while $f_1(y)$ and $f_2(z)$ are the ground-state eigenfunctions of the square-well potentials $V_1(y)$ and $V_2(z)$ given by (1), respectively, and N_1 is the normalization constant. The orthogonality of this function to the 1s-like function (5) is guaranteed by the factor $(x + i\beta y)$, where β is an additional variational parameter which is supposed to vary in the region $-1 \leqslant \beta \leqslant 0$. For wires with small extension in the y-direction and for small magnetic fields β is expected to be rather close to zero. The bulk value, -1, for β will be achieved when the extension of the wire in the y direction is infinite or for sufficiently high magnetic field for any wire extension in the y-direction.

The expectation value $\langle\Psi_1|H|\Psi_1\rangle$, for Hamiltonian H given by expression (3), has the form

$$\langle\Psi_1|H|\Psi_1\rangle = \langle\Psi_1|H_0|\Psi_1\rangle - 2N_1^2 \int_{-\infty}^{+\infty} dx \int_{-\infty}^{+\infty} dy \int_{-\infty}^{+\infty} dz\, (x^2 + \beta^2 y^2) \frac{f_1^2(y) f_2^2(z)}{\sqrt{x^2 + y^2 + z^2}} \times \exp[-2(\lambda_1 x^2 + \mu_1 y^2 + \nu_1 z^2)] \tag{22}$$

where

$$\langle\Psi_1|H_0|\Psi_1\rangle = E_1 + E_2 + \lambda_1 + \frac{(1-\alpha)^2\gamma^2}{4\lambda_1} - \frac{1}{2}(4\mu_1^2 + \alpha^2\gamma^2)\frac{d}{d\mu_1}(\ln N_1^{-2}(\mu_1, \nu_1))$$

$$-2\nu_1^2\frac{\mathrm{d}}{\mathrm{d}\nu_1}(\ln N_1^{-2}(\mu_1,\nu_1)) + N_1^2\frac{\pi^{1/2}}{(2\lambda_1)^{1/2}}$$
$$\times\left\{\left[\frac{1}{2}+\beta^2+\frac{(1-\alpha)^2\gamma^2}{8\lambda_1^2}+\frac{(1-\alpha)\beta\gamma}{2\lambda_1}\right]I_1(\mu_1)I_2(\nu_1)\right.$$
$$\left.-[-2\beta^2\mu_1+\alpha\beta\gamma]\frac{\mathrm{d}I_1(\mu_1)}{\mathrm{d}\mu_1}I_2(\nu_1)\right\} \tag{23}$$

and

$$N_1^{-2}=\frac{\pi^{1/2}}{(2\lambda_1)^{1/2}}\left[\frac{1}{4\lambda_1}I_1(\mu_1)I_2(\nu_1)-\frac{1}{2}\beta^2\frac{\mathrm{d}I_1(\mu_1)}{\mathrm{d}\mu_1}I_2(\nu_1)\right]. \tag{24}$$

$I_1(\mu_1)$ and $I_2(\nu_1)$ represent integrals defined by the formulae (14) and (15). The variational parameter α defines the gauge of the vector potential (2), as in the case of the ground state. Its value obtained for the $2p^-$ excited state is in general different from that obtained for the 1s state. This difference of the gauges of the vector potential must be taken into account when calculating the transition probability between 1s and $2p^-$ states.

The calculated energies of the dipole optical transitions from the ground to the lowest $2p^-$-like excited state are expressed by the formula

$$\Delta E=\langle\Psi_1|H|\Psi_1\rangle-\langle\Psi|H|\Psi\rangle. \tag{25}$$

The results of transition energies as a function of magnetic field are plotted in figures 4–6. Figure 4 gives the transition energies for the quantum wires for which the binding energies are presented in figure 1, while figures 5 and 6 give the transition energies for the wires whose binding energy results are presented in figures 2 and 3, respectively. The first general observation we can make is that when the extension of the wire in the direction perpendicular to the magnetic field, $l_\perp$, fulfills the relation $l_\perp \leqslant 1.5\ a_B^*$, then for $\gamma \leqslant 5$ the transition energy seems to be rather weakly dependent on the magnetic field. This situation changes for $l_\perp \geqslant 2\ a_B^*$, but nevertheless the dependence of the transition energy on the magnetic field in the considered range of γ is much weaker than that of the ionization energy. This remains true even for the bulk material (see figure 4). In figure 5 we can observe that for the wire with a small extension in the direction perpendicular to the magnetic field the slope of the transition energy as a function of magnetic field seems to be almost constant and independent of $l_\parallel$. The essential effect of the change of $l_\parallel$ seems to consist in the uniform vertical shift of the curves (see continues curves). When $l_\perp$ becomes bigger the effects of the $l_\parallel$ parameter and the magnetic field in determining the slope of the curves start to play some role for continuous curves (figure 6) and become evident for the broken curves as we can see in figures 5 and 6. In comparison to the bulk materials and to the quantum well structures the quantum wires offer not only much higher values of the 1s–$2p^-$ transition energies but also greater variety of magnetic field dependences of these transition energies with ranges of positive and negative slopes depending on the wire geometry.

In the case of a quantum wire with parabolic confinements the following variational wavefunction orthogonal to the ground-state wavefunction (20) was proposed:

$$\Psi_1'=N_{1p}(x+\mathrm{i}\beta y)\exp(-\lambda_1 x^2-\mu_1 y^2-\nu_1 z^2). \tag{26}$$

We performed the numerical calculations of the transition energy form the ground to the $2p^-$-like excited state (ΔE_p) for wires with parabolic confinements given by the same η values as in the case of the D^0 ground state ($\eta = 50$, 5.5, 0.45). All combinations of these η values were considered; this means $\eta_\perp = 50$, $\eta_\parallel = 50$; $\eta_\perp = 50$, $\eta_\parallel = 5.5$ and so on. Comparing these results with the results for corresponding rectangular quantum wires (using the correspondence established for the case of binding energy) we found that for rectangular

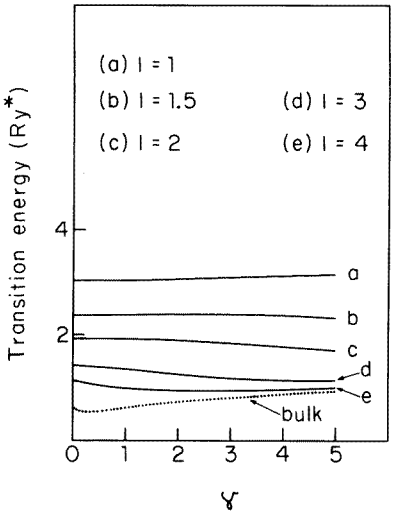

Figure 4. The transition energy from 1s to $2p^-$ states of a D^0 centre on the axis of various quantum wires with square cross section ($l_\perp = l_\parallel = l$) as a function of magnetic field. The dotted curve corresponds to the case of bulk transition energy.

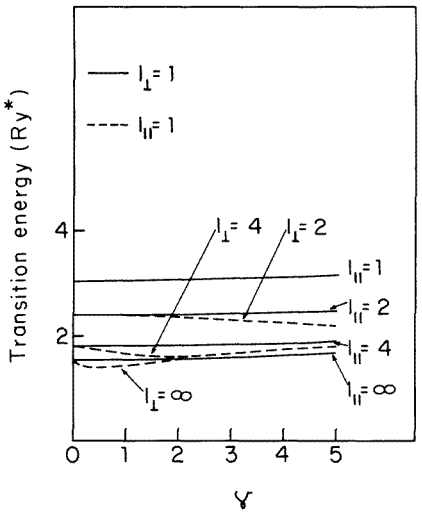

Figure 5. The transition energy from 1s to $2p^-$ states of a D^0 centre on the axis of various quantum wires with rectangular cross section as a function of magnetic field. The continuous curves correspond to the fixed length of the rectangle side $l_\perp = 1\ a_B^*$ and the broken curves correspond to the case of fixed $l_\parallel = 1\ a_B^*$.

wires with $l_\perp \leqslant 1\ a_B^*$ and $l_\parallel \leqslant 2\ a_B^*$ the relative difference between ΔE_p and ΔE given by (25) is less than 1% for the entire range of magnetic fields ($0 \leqslant \gamma \leqslant 5$). For larger values of $l_\perp$ or $l_\parallel$ this difference grows with the magnetic field but is still less than 3% for $\gamma \leqslant 2$ and less than 10% for $\gamma \leqslant 5$ (at least for $l_\perp$, $l_\parallel \leqslant 4\ a_B^*$, which were the values we considered).

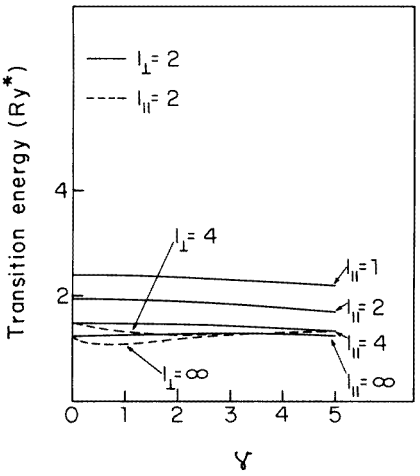

Figure 6. The transition energy from 1s to $2p^-$ states of a D^0 centre on the axis of various quantum wires with rectangular cross section as a function of magnetic field. The continuous curves correspond to the fixed length of the rectangle side $l_\perp = 2\ a_B^*$ and the broken curves correspond to the case of fixed $l_\parallel = 2\ a_B^*$.

Concluding, we can say that a rectangular quantum wire with rather small cross section but for quite a large range of magnetic fields (or a wire with larger cross sections but for small magnetic fields) can be substituted by some quantum wire with parabolic confinements if we are interested in the D^0 binding energy and the 1s–$2p^-$ transition energy.

4. Summary

We have investigated mainly the effect of the transversal dimensions of a rectangular quantum wire on the dependence of the binding energy and the dipole optical transition energy on an external magnetic field parallel to one side of the rectangle. The effect of the magnetic field on the D^0 binding energy can be quite big and is determined mainly by the dimension of the quantum wire in the direction perpendicular to the magnetic field; the dimension of the other rectangle side co-determines the magnitude of the binding energy. When the dimension of the wire in the direction perpendicular to the magnetic field is small enough the D^0 binding energy is practically independent of the magnetic field (in the range of magnetic fields we considered).

The dipole optical transition energy is weakly dependent on the external magnetic field but quantum wires offer greater variety of magnetic field dependences than bulk materials and quantum well structures.

A rectangular quantum wire can be substituted by some quantum wire with parabolic confinements if we are interested in the D^0 binding energy and the dipole optical transition energy as a function of an external magnetic field.

Acknowledgment

The author would like to thank Professor Jan Blinowski for valuable discussions.

References

[1] Sakaki H 1980 *Japan. J. Appl. Phys.* **19** L735
[2] Petroff P M, Gossard A C, Logan R A and Wiegmann W 1982 *Appl. Phys. Lett.* **41** 635
[3] Fowler A B, Hartstein A and Webb R A 1982 *Phys. Rev. Lett.* **48** 196
[4] Cibert J, Petroff P M, Dolan G J, Pearton S J, Gossard A C and English J H 1986 *Appl. Phys. Lett.* **49** 1275
[5] Temkin H, Dolan G J, Panish M B and Chu S N G 1987 *Appl. Phys. Lett.* **50** 413
[6] Tanaka M and Sakaki H 1988 *Japan. J. Appl. Phys.* **27** L2025
[7] Tsuchiya M, Gaines J M, Yan R H, Simes R J, Holtz P O, Coldren L A and Petroff P M 1989 *Phys. Rev. Lett.* **62** 466
[8] Plaut A S, Lage H, Grambow P, Heitmann D, von Klitzing K and Ploog K 1991 *Phys. Rev. Lett.* **67** 1642
[9] Calleja J M, Goñi A R, Dennis B S, Weiner J S, Pinczuk A, Schmitt-Rink S, Pfeiffer L N, West K W, Müller J F and Ruckenstein A E 1991 *Solid State Commun.* **79** 911
[10] Hiruma K, Katsuyama T, Ogawa K, Koguchi M, Kakibayashi H and Morgan G P 1991 *Appl. Phys. Lett.* **59** 431
[11] Morgan G P, Ogawa K, Hiruma K, Kakibayashi H and Katsuyama T 1991 *Solid State Commun.* **80** 235
[12] Weman H, Potemski M, Lazzouni M E, Miller M S and Merz J L 1996 *Phys. Rev.* B **53** 6959
[13] Lee J and Spector H N 1984 *J. Vac. Sci. Technol.* B **2** 16
[14] Bryant G W 1985 *Phys. Rev.* B **31** 7812
[15] Brum J A 1985 *Solid State Commun.* **54** 179
[16] Brown J W and Spector H N 1986 *J. Appl. Phys.* **59** 1179
[17] Gold A and Ghazali A 1990 *Phys. Rev.* B **41** 7626
[18] Csavinszky P and Oyoko H 1991 *Phys. Rev.* B **43** 9262
[19] Porras Montenegro N, López-Gondar J and Oliveira L E 1991 *Phys. Rev.* B **43** 1824
[20] Chuu D S, Hsiao C M and Mei W N 1992 *Phys. Rev.* B **46** 3898
[21] Porras-Montenegro N 1993 *J. Phys. C: Solid State Phys.* **5** A367
[22] Branis Spiros V, Li Gang and Bajaj K K 1993 *Phys. Rev.* B **47** 1316
[23] Dong Bin and Wang You-Tong 1994 *Solid State Commun.* **89** 13
[24] Jan J F and Lee Y C 1994 *Phys. Rev.* B **50** 14 647
[25] Brownstein K R 1993 *J. Phys.* B **26** L209
[26] Tran Thoai D B 1992 *Solid State Commun.* **81** 945
[27] Deng Zhen-Yan and Gu Shi-Wei 1993 *Phys. Lett.* **174A** 320
[28] El-Said M and Tomak M 1992 *Phys. Status Solidi* b **171** K29
[29] Oliveira L E, Porras-Montenegro N and Latgé A 1993 *Phys. Rev.* B **47** 13 864
[30] Blinowski J and Szwacka T 1994 *Phys. Rev.* B **49** 10 231
[31] Szwacka T, Blinowski J and Betancur J 1995 *J. Phys. C: Solid State Phys.* **7** 4489
[32] Fraizzoli S, Bassani F and Buczko R 1990 *Phys. Rev.* B **41** 5096
[33] Blinowski J and Kacman P 1988 *Acta Phys. Pol.* A **73** 315